

Diffusive methods of isotope separation in plasma

D A Dolgolenko, E P Potanin

DOI: <https://doi.org/10.3367/UFNe.2021.10.039094>

Contents

1. Introduction	182
2. General concepts of the theory of isotope separation in gas and plasma phases	183
3. Analysis of separation processes in systems with a traveling magnetic field	184
4. Separation of isotopes in DC discharges	187
5. Plasma centrifuges	188
5.1 Plasma dynamics and centrifugal separation in systems with crossed constant electric and magnetic fields;	
5.2 Miscellaneous separation mechanisms; 5.3 Enhancement of radial separation effects along the height of the	
discharge chamber of a plasma centrifuge with crossed fields; 5.4 High-frequency plasma centrifuges	
6. Energy consumption of diffusive plasma methods	192
7. Conclusion	193
References	193

Abstract. Studies of the separation of stable isotopes in plasma are reviewed with a focus on diffusive separation methods. The efficiency of enrichment processes is analyzed using a unified approach to the calculation of diffusive separation processes in a weakly ionized plasma. Various separation mechanisms are discussed, including centrifugal techniques, diffusive friction, thermal diffusion, and isotope cataphoresis. Results of calculations and experiments are compared. Various plasma separation devices are reviewed, and the values of specific energy consumption in different methods are compared. A conclusion is made that plasma separation methods, despite relatively high energy consumption, can be competitive in the case of elements that do not have volatile compounds under normal conditions, for which state-of-the-art centrifugal cascades cannot be used.

Keywords: stable isotopes, plasma, isotope separation, centrifugal effect, ionic wind, thermal diffusion, isotope cataphoresis, separation effect enhancement

1. Introduction

The separation of isotopes is an intrinsic area of modern industrial production that serves medicine, agriculture, science, and nuclear power engineering. Without some isotopes, it is not possible to carry out large-scale nuclear physics research in basic physics or to develop the nuclear power industry and improve its efficiency and safety.

Currently available methods for separating isotopes were originally designed primarily to obtain uranium isotopes [1].

Gaseous diffusion and centrifugation were used to this end. The essential point for these technologies is that gaseous compounds of uranium (UF_6) can be obtained under normal conditions. Gas centrifuges can also be used to produce stable isotopes [2–4]. However, most elements do not have convenient gaseous compounds, due to which the centrifugal technique, while being an economically advantageous separation method, fails to provide the production of many isotopes. This refers primarily to elements of the first and second groups and to rare-earth elements. On the other hand, the virtually universal electromagnetic method [5] is not sufficiently efficient or inexpensive.

Research and development of new separation methods is driven not only by the need to expand the range of isotopic products but also by increasingly stringent environmental requirements, since a number of isotopes are produced using environmentally harmful components. These factors triggered the development of alternative, in particular plasma, separation methods.

Isotopes of any metal elements, including refractory ones, can be obtained in plasma. However, due to fairly high energy consumption, they apparently can only be competitive in the case of elements that do not have volatile compounds under normal conditions. It should be noted that, in evaluating the economic feasibility of a particular method, capital investment should be taken into account in addition to energy costs. However, a comparison of the cost of enriching a product by different techniques is beyond the scope of this review.

Plasma methods can be conditionally divided into two groups, referred to as ‘diffusive’ and ‘selective.’ The former group includes techniques in which, similar to conventional methods (gas diffusion, thermal diffusion, and centrifugation), separation occurs due to the selective action of force fields, while the separation per se of a product occurs due to the mutual diffusion of mixture components, from which the term ‘diffusion’ originates. These include plasma methods implemented in gas-discharge systems with a traveling magnetic wave [6], direct DC discharge [7], and plasma

D A Dolgolenko, E P Potanin

National Research Center Kurchatov Institute,
pl. Akademika Kurchatova 1, 123182 Moscow, Russian Federation
E-mail: Dolgolenko_DA@nrcki.ru

Received 11 August 2021, revised 5 October 2021
Uspekhi Fizicheskikh Nauk 193 (2) 192–205 (2023)
Translated by M Zh Shmatikov

centrifuges [8]. The second group includes the ion cyclotron resonance method (ICR heating) [9, 10]. In this separation method, one of the ionic components is heated first in an isotopically selective way, and then components are separated due to the difference in the physical properties of the heated and ‘cold’ components. A detailed review of ICR studies is reported in [11]. We discuss below only plasma diffusive methods of isotope separation, which are characterized by relatively high densities of the mixture being separated, and endeavor to explore the physics of various separation mechanisms and energy costs on the basis of a unified approach.

The design of plasma gas-discharge systems is usually simpler and their manufacture is less expensive than those of ICR facilities. However, their energy costs per separation work unit (SWU) can be relatively high. In all devices of this type, the separation effect is related to the differences among the forces acting on the molecular particles of the components being separated by a certain force field under conditions of relatively high pressures of the mixture, when the separation process occurs due to the mutual diffusion of these components.

2. General concepts of the theory of isotope separation in gas and plasma phases

Before proceeding to the description of specific separation processes in diffusive-type gas-discharge systems, the general concepts of the theory of separation of gas mixture components should be outlined. The essence of the task is to separate atoms or molecules of one type from particles of another type or to provide partial separation, when the signs of deviations of the component concentrations from the original values are different in opposite zones of the device. Usually, in the ‘standard’ (if this term is applicable) separation scheme, in which the binary mixture being separated is a gas, an external selective force is applied that tends to spatially separate molecules of different types. This process is hindered by the thermal motion of the particles that suppresses the separating effect. We now consider a straight cylinder of length L filled with a binary gaseous isotopic mixture, in which molecules move in a chaotic way. We assume that a certain temperature T can be attributed to the gas. Let the molecules of both types be subjected to unequal forces f_1 and f_2 , such that $f_1 - f_2 \ll f_1, f_2$, which act in the direction of the cylinder axis (coordinate z). This inequality is typical of isotopic mixtures. We designate the mole-fractional concentration of one of the components (for example, the first one) as $C = n_1/(n_1 + n_2)$, where n_1 and n_2 are numerical densities. The initial result of the external force action is a fairly rapid emergence of a pressure gradient in the mixture. Diffusive separation develops much more slowly. It follows from the Boltzmann distribution that the equilibrium state attained at $t \rightarrow \infty$ is characterized by the presence of a concentration gradient $(dC/dz)_{eq}$, which arises due to the redistribution of components along the z -axis in the process of mutual diffusion. Diffusion transport is related to the lack of equilibrium at the initial moment after the force field is enabled, provided $f_1 \neq f_2$ [12–14]. The diffusion flux density after the establishment of the pressure gradient can be estimated as

$$j_1 = -\frac{p}{(n_1 + n_2)a_{12}} \left[\frac{dC}{dz} - \alpha_f \frac{1}{p} \frac{dp}{dz} C(1 - C) \right], \quad (1)$$

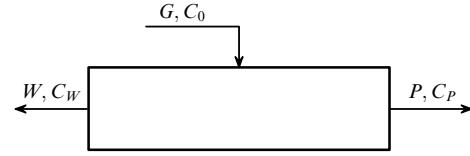


Figure 1. Schematic of a separating element.

where α_f is the barodiffusion factor,

$$\alpha_f = \frac{f_1 - f_2}{f_1 C + f_2(1 - C)},$$

p is the pressure of the mixture, and a_{12} is the coefficient that determines the force of diffusion friction between the components [15]. Below, in considering various separation mechanisms and evaluating enrichment effects, we refer to the ‘diffusive’ model described by Eqn (1).

In the equilibrium state ($j_1 = 0$), the separation factor of the isotopic mixture, defined as the ratio of the relative concentrations of the components at both ends of the separation zone at $z = L$ and $z = 0$, has the form

$$\alpha_{eq} = \left(\frac{C}{1 - C} \right)_{z=L} \left(\frac{C}{1 - C} \right)_{z=0}^{-1} = \exp \frac{(f_1 - f_2)L}{k_B T}, \quad (2)$$

where k_B is the Boltzmann constant.

It should be noted that the value of the equilibrium separation factor per se cannot fully characterize the effectiveness of the method. The initial separated mixture is added to the continuously operating element, while heavy and light fractions are taken away (Fig. 1). Therefore, it is important to obtain not only a high separation factor but also a significant flow of the selected valuable component. However, the separation factor decreases with increasing selection, which results in the existence of optimal operating modes of the separating element and such a characteristic of this element that takes into account both the degree of separation and the rate with which the original product is processed.

The separating element can be characterized by the mass flow of the initial mixture G with concentration C_0 and by the flow of selection P and waste W with concentrations C_P and C_W , respectively. As a generalized characteristic of the separation process, the concept of ‘separation power’ or ‘separation capacity’ is introduced. Studies [16, 17] suggest an energy-based approach to the interpretation of the ‘separation work’ concept. Based on this concept, the mechanical power developed by the separating element at low levels of separating effects can be estimated as

$$P_m = \frac{k_B T N_A}{2\mu} [P\Phi(C_P) + W\Phi(C_W) - G\Phi(C_0)], \quad (3)$$

where N_A is Avogadro’s number, μ is the average molecular weight of the isotopic mixture, and $\Phi(C) = (2C - 1) \times \ln[C/(1 - C)]$ is the Dirac–Peierls potential. It should be noted that the mechanical power P_m does not coincide with the minimal value required, which is usually associated with a decrease in the gas mixture entropy during separation, which is a finite separation into pure components, and therefore cannot serve as a measure of the separation work. In calculating the sum of inter-stage flows in the theory of ideal separating cascades, the ‘separating power’ value is intro-

duced in accordance with the formula [1]

$$\Delta U = P\Phi(C_P) + W\Phi(C_W) - G\Phi(C_0), \quad (4)$$

which, up to a constant factor, coincides with the mechanical power P_m . If the number of elements in an ideal cascade N is defined as the ratio of the total mechanical power consumed for the separation in the cascade to the power developed by a separate element, due to factor $k_B TN_A/(2\mu)$ being canceled out, we arrive at the formula known from the theory of cascades

$$N = \frac{\Delta U}{\delta U}, \quad (5)$$

where δU is the separating power of the element. Thus, if the separation factor α , introduced on the basis of force relations, characterizes the law of conservation of momentum and enables determination of the total number of steps in the cascade, the separation power ΔU is associated with a change in energy and makes it possible to estimate the required total number of elements in an ideal cascade with a reduction in flows between stages.

It should be noted that the separating power ΔU determines the cost of the enriched product; its value in 1 kg s^{-1} units was called the separation work unit per second (SWU s^{-1}).

3. Analysis of separation processes in systems with a traveling magnetic field

The term plasma is usually applied to the state of matter in which charged particles — electrons and ions — play the key role; this does not imply, however, that they predominate in a quantitative way. The concentration of charged particles in a weakly ionized plasma can be a relatively small fraction of the total number of particles. Should this be the case, the degree of medium ionization can be referred to as low. An important feature of plasma is its quasi-neutrality, which implies that the average number of positive and negative charges is virtually the same. If the temperature of an ordinary gas is continuously increased, sooner or later it turns into a plasma. To obtain a significant degree of ionization in a thermodynamically equilibrium and sufficiently dense medium, a very high temperature must be maintained. However, in research laboratories, plasma has long been created under thermally nonequilibrium conditions in so-called gas-discharge systems, which are vessels or tubes filled with gas at a relatively low pressure and in which constant or alternating electric fields are excited. In this case, a sufficiently high concentration of charged particles is attained due to heating of the electronic component in electric fields rather than an increase in the neutral gas temperature. An ordinary neutral gas always contains a certain amount of so-called seed electrons (produced, for example, by cosmic radiation). The acceleration of seed electrons by external electric fields leads to an avalanche ionization of the gas and its breakdown. Since the probability of electron impact ionization is relatively high, a relatively high degree of ionization can be maintained after breakdown at a low electron temperature. The temperature of neutral particles is in this case even lower. The described ionization mechanism can be called ‘nonequilibrium.’ Depending on the way an electric field is applied to the discharge gap, high-frequency (HF) and DC discharges are distinguished. Since energy losses are of importance in the

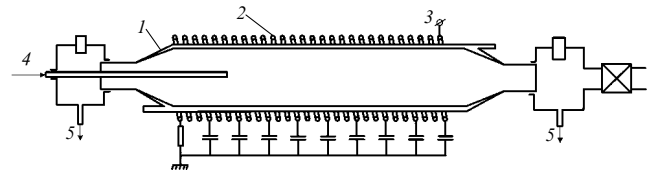


Figure 2. Block setup of a device with a traveling magnetic wave.

separation of isotopes, it is reasonable to use weakly ionized plasma, the cost of obtaining which is minimal.

Interest in the study of separation processes in plasma is associated with the problems of obtaining isotopes of elements that do not have convenient gaseous compounds at room temperature. We consider below enrichment of isotopic mixtures in HF gas-discharge systems with a traveling magnetic wave, which, as seen in Fig. 2, comprise a long cylindrical water-cooled chamber (1) filled with a mixture to be separated, along which coils with specially phased HF electric currents (2) are located, which create a traveling magnetic wave. The delay line is powered by an HF generator (3). The HF electromagnetic field excited by the coils inside the chamber ignites a discharge in the mixture and exerts a force on the generated plasma in the longitudinal direction. The figure also shows the inlet system (4) and chamber evacuation device (5). The action of a traveling magnetic field can be visually illustrated as a conductive medium placed between the tips of a permanent magnet that moves in the direction of the z -axis (Fig. 3). The moving magnetic field, as it were, entrains the plasma in the axial direction. In physical terms, such entrainment of the plasma is explained by the fact that the currents which flow in it interact with the magnetic field, and a component of the volume electromagnetic force arises in the direction of the magnet movement F_z :

$$F_z = [\mathbf{J}, \mathbf{B}]_z, \quad (6)$$

where \mathbf{J} is the electric current density and \mathbf{B} is the magnetic induction.

In the case under consideration of a gas-discharge system with a traveling magnetic field, the force averaged over a period acts on a conducting medium as a result of the interaction of the time-variable azimuthal current and the radial magnetic field. Should chamber 1 have no ends (i.e., it would be a toroidal closed system), a unidirectional hydrodynamic flow alone would arise in the stationary state. Due to the presence of ends, the average flow through the cross section is zero. In this case, a longitudinal pressure gradient

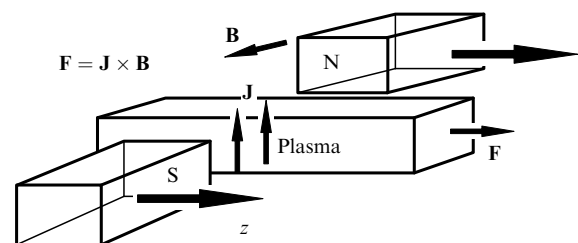


Figure 3. Mechanism of plasma entrainment by a moving magnetic field. \mathbf{J} is the electric current density, \mathbf{B} is the magnetic induction, \mathbf{F} is the force ‘pushing’ the plasma as a whole along the z -axis.

and a corresponding redistribution of the gas density emerge. The first experiments with a traveling magnetic field carried out by R A Demirkhanov et al. [6] showed that noticeable longitudinal separation effects exist in both gaseous and isotopic mixtures. The mixture was enriched with a heavy component in the high pressure region. Since the reasons for such a redistribution of concentration along the system length in isotopic mixtures were unclear, it was of utmost importance to understand the separation mechanisms. To this end, experiments were carried out under the guidance of I K Kikoin at the Kurchatov Institute of Atomic Energy (IAE) that revealed the main separation processes in systems with a traveling magnetic wave [18–20].

Initially, it was assumed in [6] that it is the occurrence of a pressure drop in the mixture that leads to the separation due to so-called *barodiffusion* in the Chapman–Cowling terminology [21]. Enrichment should be proportional in this case (with not very large differences Δp) to the ratio $\Delta p/\langle p \rangle$ ($\langle p \rangle$ is the average pressure in the discharge), the heavy component being concentrated in the area of increased pressure. Experiments confirmed the existence of a longitudinal separation process and the predominant transport of heavy isotopes in the direction of wave propagation (or a high pressure zone). However, the barodiffusion-based dependences failed to describe the magnitudes of enrichment effects. An analysis of the experimental data and their comparison with the results of various computational models made it possible not only to determine the mechanisms for the separation of isotopic and gaseous mixtures but also to clarify the meaning of the very concept of *barodiffusion*.

First of all, it has been shown that processes of the barodiffusion type in Chapman–Cowling terminology can only occur in the case of purely mass force fields and, as applied to a separating device with a traveling magnetic wave, are not substantiated in any way. Therefore, it was initially suggested that the observed separation effects are related to radial thermal diffusion, which is converted into a longitudinal effect due to circulation. Indeed, as a result of the cooling of the discharge chamber walls, a radial temperature gradient appeared in the gas and, as a consequence, corresponding thermal diffusion separation occurred. Studies [18, 19] provided a description of the physical effects in the system associated with radial separation in the discharge, the occurrence of a longitudinal pressure drop, and circulation flow $V_z(r)$ due to the radial inhomogeneity of the longitudinal electromagnetic force acting on the plasma $\langle F_z \rangle$ averaged over the field period (Fig. 4). The calculation results were compared with experimental data [20]. Xenon was used as the working gas in the experiments. In Fig. 5, the solid line shows the calculated pressure drop Δp along the device length

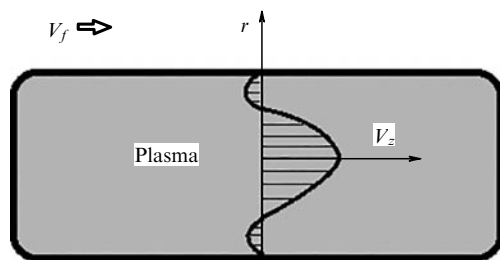


Figure 4. Circulation of an isotope mixture in a system with a traveling magnetic field.

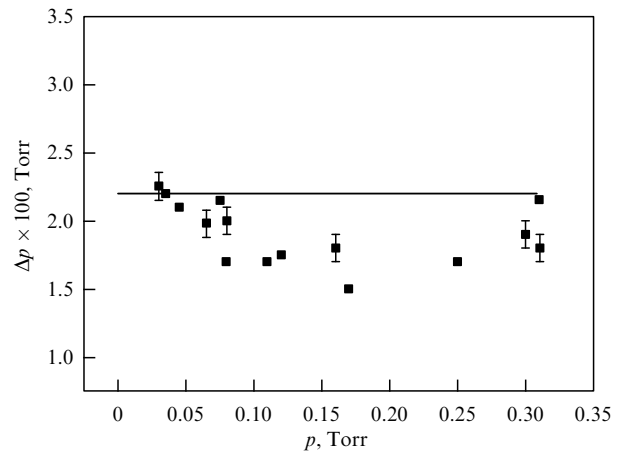


Figure 5. Longitudinal pressure drop Δp as a function of the initial pressure in chamber p . Working gas Xe, phase velocity of the traveling wave $V_f = 1.2 \times 10^5$ m s⁻¹, power input into the plasma $W = 2.8$ kW. Solid line shows calculation results.

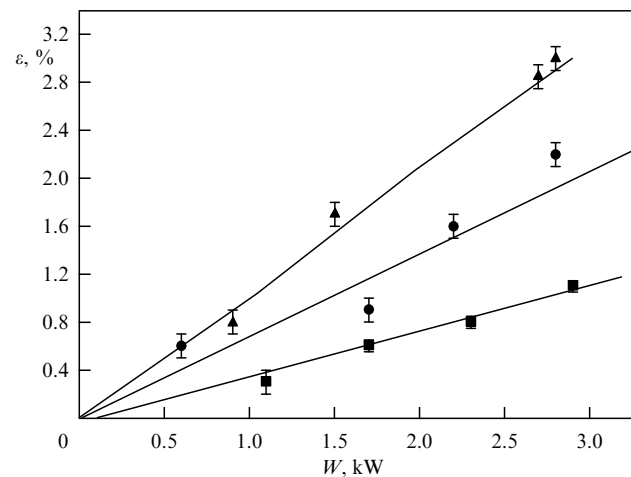


Figure 6. Enrichment factor ε as a function of power W for different initial pressures in chamber p . Triangles— $p = 6.0 \times 10^{-2}$ Torr, squares— $p = 1.6 \times 10^{-1}$ Torr, and dots— $p = 3.2 \times 10^{-1}$ Torr. Solid lines show the result of approximations.

as a function of the initial pressure in the chamber p . Squares represent experimental data. The pressure drop magnitude determines not only the efficiency of the longitudinal force action on the isotopic mixture but also the intensity of the hydrodynamic circulation flow, which leads to the enhancement of the primary radial thermal diffusion along the discharge chamber length. Separation effects were experimentally studied using a mixture of xenon isotopes: 50% ¹³⁶Xe–44% ¹²⁹Xe–6% ¹²⁸Xe. Figure 6 shows the dependence of the enrichment factor $\varepsilon = (C_p^{136} - C_0^{136}) / C_0^{136}(1 - C_0^{136})$ on the power W input into the discharge for various pressures p . Solid lines show the results of approximating experimental data. As can be seen, the power dependence of the effect is close to linear. Figure 7 shows the experimental and calculation data as a function of pressure on a logarithmic scale. Dashed-dotted curve 1 shows the dependence of the longitudinal enrichment factor ε on pressure for barodiffusion in Chapman–Cowling terminology. As can be seen, this dependence fails to reproduce the experimental results (shown by dots) in even qualitative

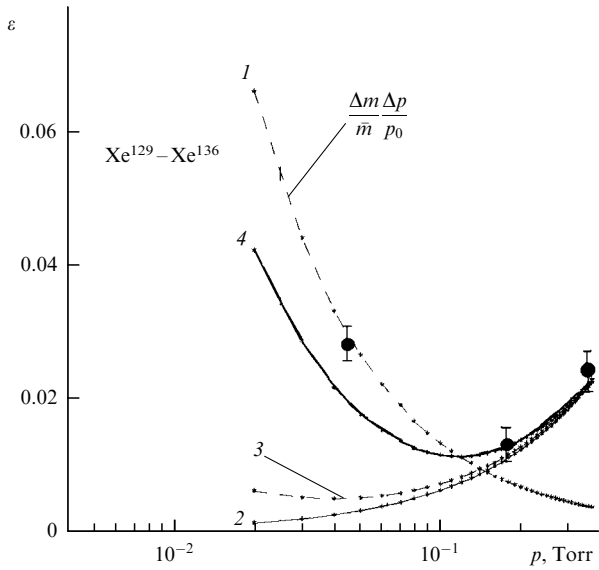


Figure 7. Coefficient of enrichment of a quasi-binary Xe isotopic mixture as a function of pressure. Curve 1—theory ('barodiffusion'), curve 2—theory (thermal diffusion enhanced due to electromagnetic convection), curve 3—theory (thermal diffusion + 'ionic wind'), curve 4—theory taking into account thermal diffusion, ionic wind, and the differences among the degrees of isotope ionization; dots show the results of the experiment [18].

terms. The discrepancy is especially pronounced at high pressures. However, while an assumption that in this case radial thermal diffusion alone, enhanced by 'electromagnetic convection,' is operative provides an explanation for the experimental data in the high pressure region (curve 2); at low pressures, it yields a greatly underestimated result for the longitudinal coefficient enrichment.

It should be noted that a significant consequence of the longitudinal action of a traveling electromagnetic wave on the plasma, especially at significant values of input power, is the formation of compression and depression zones in the discharge. Apparently, the processes of ionization and recombination proceed in these zones in different ways. If ionization prevails in the low-pressure zone, then, in addition to the radial flow, there is a longitudinal ambipolar flow of charged particles into the high-pressure zone, in which recombination predominates. The presence of a longitudinal flow of ions, in turn, can lead to the emergence of separation effects in the neutral component of the plasma. One of these effects is associated with the difference in the magnitude of the longitudinal forces of diffusion friction of ions against neutral particles of different types. The nature of this mechanism, referred to as the *ionic wind*, is similar to that of the mass-diffusion effect in ordinary gas mixtures [22, 23]. The underlying mechanism is that, in the case of an elastic collision of two particles, the momentum transferred is proportional to the first power of their reduced mass, as a result of which a heavy neutral particle at each collision with an incident ion transfers a larger momentum than a light one does. As a result, a large average force of diffusive friction acts on the heavy neutral component from the side of the ion flow, which leads to the emergence of a nonequilibrium state and separation. We now consider a binary mixture and denote by n_1 and n_2 the densities of type-1 and type-2 ions, by n_3 and n_4 the corresponding densities of neutral particles, and by \mathbf{V}_j the macroscopic velocity of particles of the j th type. In

calculating the diffusive friction forces in the case of purely isotopic mixtures, the effect of resonant charge exchange should be taken into account [24, 25]. In this case, the structure of formulas for the diffusive friction forces differs from the usual one characteristic of purely elastic interactions. For example, while the friction force acting on a neutral component of type 1 in elastic collisions with ions of both types is described by the formula

$$\mathbf{R}_3 = n_1 n_2 a_{13} (\mathbf{V}_1 - \mathbf{V}_3) + n_2 n_3 a_{23} (\mathbf{V}_2 - \mathbf{V}_3), \quad (7)$$

where a_{ij} are the diffusive friction coefficients, in the case of pure charge exchange, it is determined as

$$\mathbf{R}_3 = \mathbf{R}_3^{3-1} + \mathbf{R}_3^{1-4} + \mathbf{R}_3^{3-2}, \quad (8)$$

where $\mathbf{R}_3^{3-1} = n_1 n_3 a_{13}^* (\mathbf{V}_1 - \mathbf{V}_3)$ corresponds to the loss and gain of momentum due to charge exchange collisions between intrinsic components, $\mathbf{R}_3^{1-4} = n_1 n_4 a_{14}^* \mathbf{V}_1$ characterizes the momentum gain due to the appearance of type-1 neutral particles due to the charge exchange of type-1 ions on type-2 neutral particles, and $\mathbf{R}_3^{3-2} = -n_3 n_2 a_{32}^* \mathbf{V}_3$ corresponds to the loss of momentum due to the disappearance of type-1 neutral particles as a result of the recharging of type-2 ions on type-1 neutral particles.

The difference between the structures of Eqns (7) and (8) results in a fundamental difference in the nature of the mass-diffusion separation of isotopes in cases where the current is transported by ions of another easily ionizable element or by intrinsic ions of the isotopes being separated [26–29].

However, it turns out that, despite the qualitatively correct dependence of the effect on pressure, in the low pressure region, taking into account the ionic wind fails to provide a quantitative agreement between theory and experiment (see Fig. 7, curve 3). This is mainly due to the fact that the charge exchange and reverse flow of neutral atoms formed as a result of the neutralization of ions in the higher pressure region reduce the effect of the ionic wind. As experiments carried out in [30] showed, in complex mixtures that consist of various isotopic and chemical components, isotopes of easily ionizable components are separated more efficiently. This observation prompted the idea of a fundamentally new separation mechanism associated with the difference among the degrees of ionization of isotopes in the discharge. By analogy with the mechanism of separation of gas mixtures with different ionization potentials, this mechanism was called 'isotopic cataphoresis' [31, 32]. Ionization potentials of isotopes are virtually the same, and differences among them cannot directly lead to any noticeable difference in the ionization degree. However, due to the unequal rate of losses of charged particles on the discharge-chamber walls, such a difference should occur. Indeed, in the process of radial ambipolar diffusion, heavy ions are subjected to a larger force of braking against a neutral gas than light ones, as a result of which their average 'lifetime' and, consequently, the degree of ionization of the heavy component turn out to be higher. In this case, the corresponding relative difference among the degrees of ionization is described by the formula

$$\frac{\Delta\beta}{\beta} \approx \frac{\Delta m}{4m} \frac{Q_{\text{in}} + 6Q_{\text{in}}^*}{(Q_{\text{in}} + 2Q_{\text{in}}^*)(1 + \Theta)}, \quad (9)$$

where Δm is the mass difference between the isotopes, $\Delta\beta = \beta_1 - \beta_2$, $\beta_1 = n_1/n_3$, $\beta_2 = n_2/n_4$, Q_{in} and Q_{in}^* are the

effective cross sections of elastic collisions and charge exchange,

$$\Theta = \frac{3T_i R^2}{x_R^2 T_e} (n_3 + n_4)^2 Q_{in}^* (Q_{in} + 2Q_{in}^*),$$

R is the discharge chamber radius, T_i and T_e are the temperature of ions and electrons, and $x_R = 2.4R$. The combined action of the longitudinal ionic mechanisms and thermal diffusion is described by the formula

$$\varepsilon \approx a \frac{\Delta m}{m} \frac{\Delta p}{\langle p \rangle}, \quad (10)$$

where

$$a \approx \frac{q_i + 3}{4(q_i + 1)^2} \left(q_i - q_n \frac{\Theta}{1 + \Theta} + \frac{1}{1 + \Theta} \right),$$

$$q_i = \frac{Q_{in}}{2Q_{in}^*}, \quad q_n = \frac{Q_{nn}}{2Q_{in}^*},$$

with Q_{nn} being the effective cross section for elastic scattering of neutral particles. It should be noted that, as applied to the parameters of setup [19, 20], the value of a varies in the range of 0.2–0.5 with an increase in pressure from 6×10^{-2} Torr to 2×10^{-1} Torr, and is not equal to unity, as should be the case according to the Chapman–Cowling theory of barodiffusion. As can be seen from Fig. 7, curve 4 qualitatively correctly reproduces the dependence on pressure and describes well the experimental data at high pressures.

In [33], the process of isotope separation in the vapor phase was studied in the stationary regime of the process. The separation of cadmium isotopes was examined. The discharge chamber consisted of two coaxially arranged quartz tubes, the gap between which was filled with zirconium oxide powder. The chamber was cooled outside by running water. Cadmium was evaporated from a special ampoule using a heater. Xenon was introduced into the chamber as a small additive. Samples were taken by condensing vapors on the cooled end surface of the probe. Enrichment factors of the order of 4% per unit mass difference were achieved. These experiments confirmed the fundamental possibility of isotope separation in the vapor phase, which is important if plasma methods are used to enrich isotopes of elements that do not have convenient gaseous compounds.

4. Separation of isotopes in DC discharges

The gas-discharge system consists of a long cylindrical water-cooled quartz chamber closed at the ends, which contains inside the gas mixture to be separated. At the chamber ends, electrodes are placed, between which a potential difference is maintained. A simplified schematic of such a device is shown in Fig. 8. In the positive column of the discharge, which occupies almost the entire volume between the electrodes, an electric current flows, which is carried primarily by electrons that move from the negative electrode (cathode) to the positive electrode (anode). However, there is also a flow of ions towards the cathode. A significant difference between a direct discharge and a system with a traveling magnetic field is that the longitudinal gradient of neutral gas pressure between the ends of the system is virtually absent. In a DC discharge, the small pressure gradient associated with the different nature of the interaction of charged particles with the chamber wall has the opposite sign. The degree of ionization in gas-discharge systems usually does not exceed a few

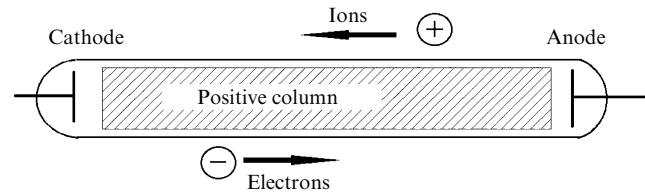


Figure 8. Schematic of a direct DC discharge.

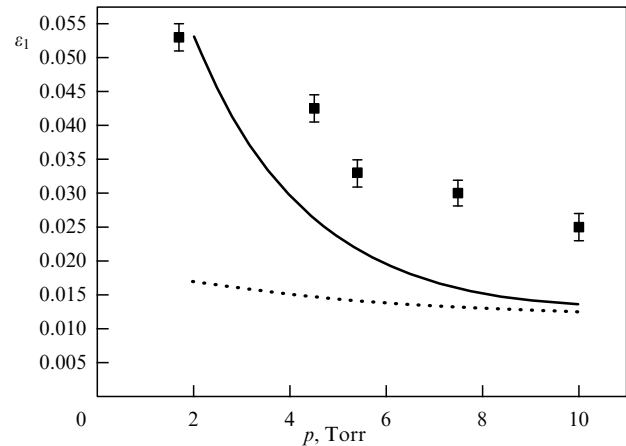


Figure 9. Enrichment factor as a function of pressure in a capillary DC discharge.

percent, and the plasma can be considered weakly ionized. It is with such a medium that we are dealing in considering separation processes in DC discharges. The successful separation of neon isotopes in a high-current direct discharge was first reported in [7]. The concentration of the mixture was measured at the ends of a capillary about 3 mm in diameter. The initial pressure in the discharge was about 3 Torr, the current density was $J = 50 \text{ A cm}^{-2}$, and the capillary length was 10 cm. A very large separation factor was observed: $\alpha \approx 1.45$ ($\varepsilon \approx 45\%$). It should be noted that, in the best industrial separation methods, the magnitude of the primary enrichment effect $\varepsilon = \alpha - 1$ usually does not exceed a few percent. The results obtained in [7] were experimentally confirmed in [34, 35]. The separation of isotopic mixtures of neon, krypton, and xenon was studied. Figure 9 shows the dependences of the enrichment factors per unit mass difference, ε_1 , on the initial pressure p in a tube with inner diameter $d \approx 3 \text{ mm}$ at a discharge current of $I_r = 10 \text{ A}$. It is worth noting that, in all experiments, it was the near-cathode zone, into which the flow of ions is directed, that was enriched with a heavy isotope, rather than the near-anode region of higher pressure. This result confirms the ideas developed above about the mechanisms of separation in a weakly ionized plasma.

The first attempt to quantitatively compare the observed separation effect with theoretical results was made in [7]. The authors of [7] based their work on the concept of the difference in momentum transferred to various neutral components from ions. In considering above the systems with a traveling magnetic field, such a mechanism was called above in our terminology the *ionic wind*. The existence of a reverse flow of neutral atoms, which is a consequence of the neutralization of ions in the near-cathode region, was not taken into account, and the role of charge exchange in the

process of momentum transfer from ions to neutral atoms was not taken into account either. Physically, the weakening of the separation effect due to the reverse flow of neutral atoms is due to the diffusive friction force acting on heavy neutral atoms in the direction opposite to the motion of ions. The two latter phenomena counteract separation, and the formula for the enrichment factor becomes

$$\varepsilon = \frac{\Delta m}{m} \frac{(Q_{\text{in}} + 6Q_{\text{in}}^*)(Q_{\text{in}} - Q_{\text{nn}})}{(Q_{\text{in}} + 2Q_{\text{in}}^*)^2} \frac{n_i e E_z L}{n k_B T_n}, \quad (11)$$

where E_z is the longitudinal component of the electric field strength in the positive column and T_n is the temperature of neutral atoms. The value of ε determined according to Eqn (11) turns out to be significantly less than the estimation of [7]. If isotopic cataphoresis is taken into account, we obtain for the enrichment factor

$$\varepsilon = \left\{ \frac{\Delta m}{4m} \frac{(Q_{\text{in}} + 6Q_{\text{in}}^*)(Q_{\text{in}} - Q_{\text{nn}})}{(Q_{\text{in}} + 2Q_{\text{in}}^*)^2} + \frac{\Delta \beta}{\beta} \frac{Q_{\text{nn}} + 2Q_{\text{in}}^*}{Q_{\text{in}} + 2Q_{\text{in}}^*} \right\} \frac{n_i e E_z L}{n k_B T_n}. \quad (12)$$

The solid curve in Fig. 9 shows the enrichment factor ε_1 calculated using Eqn (12) per unit mass difference for a natural multicomponent krypton isotope mixture in the case of a capillary with length $L = 0.17$ m. The dots represent the experimental data obtained in study [34]. The dotted curve only takes into account the action of the ‘ionic wind.’

Detailed investigations of the plasma parameters of a DC discharge in neon were carried out in [36]. Isotope separation processes were also studied in [36], and the results of experiments and calculations were compared applying the ‘ionic wind’ theory in [31, 37].

From the perspective of reducing energy consumption during separation, it is reasonable to use a longitudinal magnetic field, which reduces the losses of charged particles on the device wall. This leads to a decrease in the power input into the plasma. In [38], the influence of a longitudinal magnetic field on the separating characteristics of a DC discharge was estimated. The formula for the relative difference in the degrees of ionization of isotopes under the action of a magnetic field now has a more complex form than Eqn (9):

$$\frac{\Delta \beta}{\beta} \approx \frac{\Delta m}{4m} \frac{Q_{\text{in}} + 6Q_{\text{in}}^*}{(Q_{\text{in}} + 2Q_{\text{in}}^*)(1 + \Theta)} \times \frac{1}{1 + T_i R^2 n_n^2 Q_{\text{in}}^* (Q_{\text{in}} + 2Q_{\text{in}}^*)(1 + \chi)/3(T_e + T_i)}, \quad (13)$$

where $\chi = \gamma_e \gamma_i$, $\gamma_e = eB/(n_n \alpha_{\text{en}})$, and $\gamma_i = eB/(n_n \alpha_{\text{in}})$ are the magnetization parameters of electrons and ions. Calculations based on Eqn (13) showed that an increase in the magnetic field leads to a slight decrease in the relative difference among the isotope ionization degrees, and, consequently, in the longitudinal separation effect. This result was confirmed experimentally in magnetic fields up to the order of $B_z = 0.1$ T [39]. Thus, the use of a magnetic field can help reduce energy consumption in isotope separation, provided the energy consumed to maintain the magnetic field is small.

5. Plasma centrifuges

After the centrifugal method for the separation of stable isotopes was successfully developed in the USSR, the idea of

using a rotating plasma actively attracted the attention of foreign specialists [8, 40–42]. The interest shown was related to the possibility of achieving very high rotational speeds of the mixture and attaining enrichment factors and separating capacities greater than in a mechanical centrifuge. In addition, this method was attractive due to the simplicity of the design and the absence in it of moving parts, which are characteristic of a gas centrifuge. Later, Russia joined research on plasma centrifugation [43–46]. However, the interest in plasma centrifugation was only associated with the possibility of its application for the separation of isotopes of elements that do not have convenient gaseous compounds. The possibility of exciting centrifugal forces due to crossed constant electric and magnetic fields and a high-frequency rotating magnetic field was investigated. Study [47] explored the idea of using a rotating magnetic field in the separation of isotopes and gas mixtures for the processing of spent nuclear fuel.

5.1 Plasma dynamics and centrifugal separation in systems with crossed constant electric and magnetic fields

Initially, attempts were made to develop a plasma centrifuge based on crossed constant radial electric and axial magnetic fields. A simplified schematic of the device is shown in Fig. 10. The rotation of the mixture in this case is due to the action of the azimuthal electromagnetic force related to the interaction of the radial electric current J_r and the axial magnetic field B_z . The figure shows the characteristic profile of the azimuthal velocity of the medium, taking into consideration viscous effects on the electrodes. The most complete physical results were obtained on impulse installations, which made it possible to implement significant specific energy inputs using relatively simple means and lower the requirements for the thermal stability of construction materials. The first serious attempt to create an efficient plasma centrifuge was made by Bonnevier ([8], hydrogen isotopes). Careful measurements of separation effects in a xenon isotopic mixture

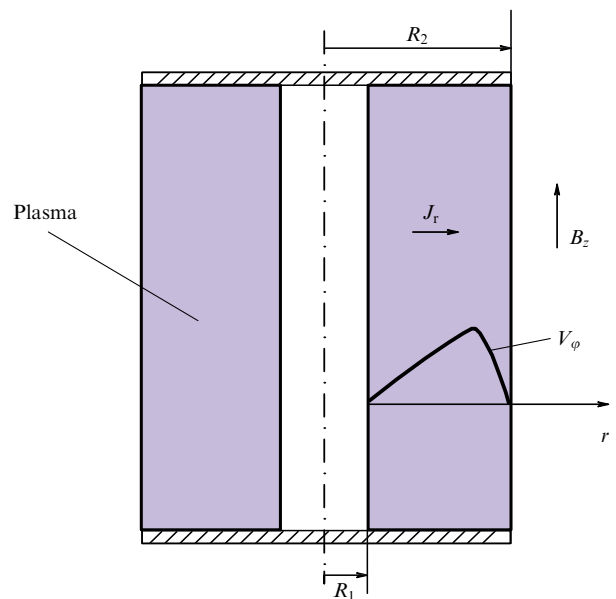


Figure 10. Simplified schematic of a plasma centrifuge with crossed fields: J_r is the density of the radial current, B_z is the induction of the longitudinal magnetic field, and R_1 and R_2 are the radii of the inner and outer electrodes.

were performed in [43, 44]. In experiment [44], where hydrogen was added to separated isotope mixtures of He and Ne, results were obtained that were record breaking for pulsed systems: the radial separation factor α_r in a natural mixture of neon reached 1.44, and for helium isotopes, it was 5.7. Separation of hydrogen–deuterium mixtures in a weakly ionized plasma was studied in [45, 46]. In [48], isotope separation in a pulsed system with crossed fields was studied at powers of the order of 1 MW input into the plasma. The radial discharge in the vacuum chamber was maintained between the central electrode (cathode) and the side surface of the chamber. The magnetic system created a longitudinal magnetic field in the discharge region. The interaction of the radial electric current and the longitudinal magnetic field brought the plasma into rotation. The experiments were carried out on various isotopic mixtures at a pressure of about 10^{-1} Torr in a wide range of currents (up to 8 kA) and magnetic fields (up to 0.6 T). Optical methods were used to measure the plasma density, the temperature of the neutral and ionic components, and the radial distribution of the rotation velocity for these components. It was found that secondary flows affect the spatial distribution of concentration in the discharge chamber.

In [49], experiments were carried to separate uranium isotopes in the plasma of a rotating arc. The discharge was created between a uranium cathode 0.8 cm in diameter and an annular anode 2 cm in diameter. The discharge chamber length reached 40 cm, the discharge current was 180 A, and the magnetic field induction was 0.8 T. The plasma rotation speed was shown to reach 2×10^3 m s $^{-1}$.

Isotope separation in a rotating plasma of a beam discharge was studied in [50]. In [51, 52], a ‘polarization’ mechanism of isotope separation was proposed, which is realized near the end of the chamber in a completely ionized plasma. In [53], positive results in the separation of nickel isotopes were obtained in a rotating plasma of metal vapors detached from the chamber walls. Studies of rotating arc plasma were continued in [54, 55]. The instabilities of a collisional rotating plasma were analyzed in [56]. It was shown that ion-cyclotron instability can develop in a rotating plasma at moderate frequencies of particle collisions. These instabilities are completely stabilized in a dense plasma.

Attempts to theoretically describe separation processes in pulsed plasma centrifuges encounter the problem of the nonstationary character of the processes. In [57], the time was calculated that is required for the establishment of the hydrodynamic rotation velocity and gradients of concentrations of the mixture being separated. An analysis of the time of establishment of the azimuthal velocity in the hydrodynamic approximation showed that, for the plasma parameters described in [43], the hydrodynamic and separation processes in plasma can be considered quasi-stationary.

5.2 Miscellaneous separation mechanisms

The centrifugal separation effect is not the only phenomenon which is observed in a plasma centrifuge. The presence of a heat source related to the flowing of electric currents and viscous dissipation results in the emergence of temperature gradients in the mixture being separated, which, in turn, generate thermal diffusion processes. In addition, in a plasma centrifuge with crossed electric and axial magnetic fields, the radial ion flow under the conditions of magnetization of the electron component causes separation effects related to the selectivity of the

transfer of momentum from ions to neutral atoms (ionic wind) [58, 59].

Since, in the version of the plasma centrifuge with an axial magnetic field under consideration, losses of charged particles from the discharge volume primarily occur along the magnetic field direction towards the chamber end, the process of longitudinal diffusion can also result in a difference between degrees of isotope ionization and, consequently, manifestation of the cataphoresis separation mechanism. Both the ionic wind and isotopic cataphoresis under positive polarity of discharge voltage (external electrode—cathode) enhance the total radial separation effect, while, if the polarity is negative, they operate opposite to the centrifugal mechanism. In study [17], a unified diffusion model was used to analyze in detail the mechanisms described, and it shows that, under certain conditions, they can make a noticeable contribution to the separation effect in addition to the centrifugal mechanism. It is worth noting that these effects were observed in specially implemented modes in experiment [43]. Furthermore, the unified diffusion model was used to examine the ‘end face’ separation mechanism, which is due to the difference between azimuthal friction forces acting on isotope ions [60, 61]. Another separation effect, related to the difference among azimuthal velocities of ions and neutral atoms, is due to the presence in the isotope mixture being separated of a third, hardly ionizable, component [62]. The enrichment coefficient can be represented then in the form

$$\varepsilon_r \approx \frac{\Delta m}{m} \frac{M}{M+m} \frac{\chi_i^2}{1+\chi_i^2} \frac{Q_{nN}}{Q_{iN}} \frac{\beta e E_r R_2}{k_B T}, \quad (14)$$

where Q_{iN} and Q_{nN} are the cross sections of elastic scattering of ions and neutral atoms of the mixture being separated on neutral atoms of the hardly ionizable component, χ_i is the ion magnetization parameter, and M is the mass of the ion of the hardly ionizable component. Enrichment, which is proportional to ionization degree, increases with the magnetic field strength.

In study [63], power consumption in plasma centrifugation was estimated for the experimental setup described in [64]. The issue of the energy consumption of plasma separation facilities is considered in detail in Section 6.

5.3 Enhancement of radial separation effects along the height of the discharge chamber of a plasma centrifuge with crossed fields

The effective use of a gas centrifuge is known to become feasible due to the creation of a countercurrent flow of heavy and light fractions. The essence of the enhancement effect is that under certain conditions in a sufficiently long column, the radial effect is enhanced along the length due to the axial circulation flow. The enhancement is associated with the transfer of heavy and light isotopes in opposite directions along the axis and their predominant accumulation in opposite near-side zones. In fact, the axial concentration gradient is associated with the action of diffusion friction forces, which are excited in the process of reverse diffusion of the components. An increase in the degree of separation in a single facility is facilitated by external cascading [1]. Since implementation of external cascading is more challenging in the case of plasma methods, the need for internal cascading for a plasma centrifuge becomes apparent. It should be emphasized that the implementation of internal cascading not only increases the degree of enrichment of the product

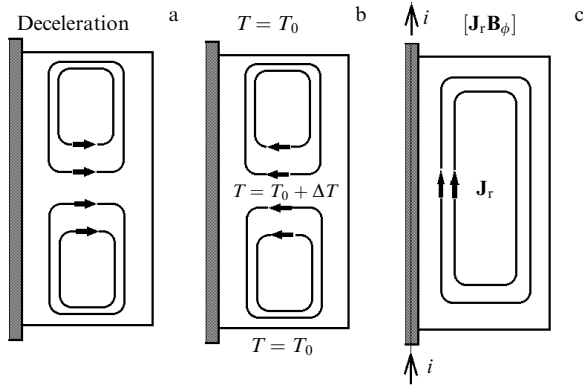


Figure 11. Schematic of excitation of circulation flows: (a) circulation due to deceleration of the gas on the end surfaces; (b) circulation due to gas cooling at the ends; (c) forced electromagnetic convection excited by an axial current-carrying rod.

with the desired isotope but also facilitates the very selection of the target component of the isotopic mixture without significant mixing of the separated components of the mixture, when the extraction and waste zones are associated with opposite ends of the column.

The circulation is excited in a mechanical centrifuge under the effect of two mechanisms: an axial temperature gradient or the mechanical braking of the rotating flow [2]. It turns out that, in a plasma centrifuge, in relation to its design features, circulation is excited in the separation chamber due to deceleration of the gas flow at its ends. Study [65] examined the reasons for the excitation of countercurrent flows associated with the action of the ends, which slow down the rotation of the plasma (Fig. 11a), and temperature gradients (symmetric excitation, the so-called thermocentrifugal effect) (Fig. 11b). As applied to the stationary mode, the efficiency of the primary effect enhancement due to the circulation caused by the internal axial current-carrying rod (Fig. 11c) was calculated. It should be noted that the excitation of circulation by decelerating ends and symmetrical cooling of the ends is inefficient due to the appearance of two vortices rotating in opposite directions (Fig. 11a and b) and a drop in the rotation speed. More promising is the use of a circuit with an axial current (Fig. 11c). It has been established in this case that no fundamental problems exist for stationary systems that would prevent implementing effective enhancement, since the estimated optimal currents in the axial rod have rather low values. Figures 12 and 13 show the calculated dependences of the optimal circulation V_1^* and the enhancement factor $K_z^* = \varepsilon_z/\varepsilon_{0r}$. The latter factor is the ratio of the longitudinal and transverse enrichment effect values from the compressibility parameter $\alpha_1^* \approx \mu V_{\varphi 0}^2/(\mathcal{R}T)$, where $V_{\varphi 0}$ is the maximum medium rotation speed and \mathcal{R} is the universal gas constant. It has been established that, with an increase in the compressibility parameter, effective enhancement can be attained by increasing the circulation. Thus, it has been confirmed that, in a plasma centrifuge, in principle, not only is the conversion of a radial effect into a longitudinal one possible, but so is its significant enhancement along the column length. The maximum enhancement factor can be estimated as

$$K_z^M = \frac{\varepsilon_z^M}{\varepsilon_{r0}} \approx 0.5 \frac{L}{R_2}. \quad (15)$$

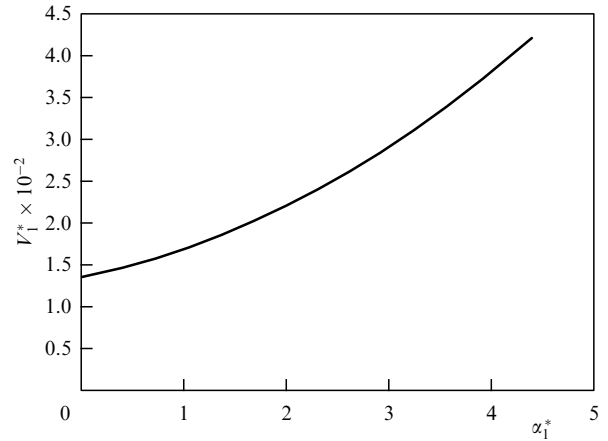


Figure 12. Optimal circulation velocity V_1^* as a function of compressibility parameter α_1^* .

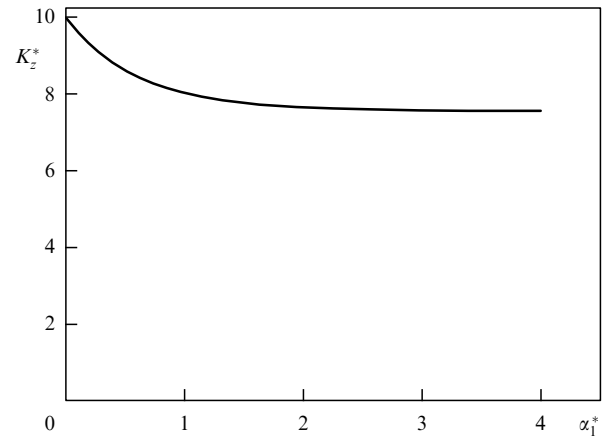


Figure 13. Enhancement factor K_z^* as a function of parameter α_1^* .

Study [57] explains, as applied to pulsed systems, the nonstationary effects of the axial redistribution of concentration, which were experimentally examined in [48, 66].

In [67], it was proposed to create a countercurrent by cooling one of the ends of the discharge chamber of a plasma centrifuge with crossed fields ($\mathbf{E} \times \mathbf{B}$) (asymmetric excitation). It has been shown that by reducing the temperature of the lower end relative to that of heavy particles of a weakly ionized plasma from 2000 K to 1000 K at medium densities $\rho_1 = 5 \times 10^{-3} \text{ kg m}^{-3}$, acceptable enhancement of the primary effect along the column height can be obtained.

5.4 High-frequency plasma centrifuges

The use of crossed constant fields for the effective excitation of a centrifugal force field was experimentally demonstrated in [44, 49, 53]. However, a number of technological problems were pointed out, related, in particular, to the presence of electrodes. In [68, 69], an alternative method for accelerating a conducting gas was proposed in which a high-frequency gas-discharge system with a rotating magnetic field was used. The inductive nature of the discharge, in contrast to that of the discharge in similar devices with crossed constant fields, made it possible not to use electrode systems. As shown experimentally in [69], as applied to the dipole configuration of the magnetic field for HF discharges in the range of field rotation frequency $\nu = 10^5 - 10^7 \text{ Hz}$ with a real energy input

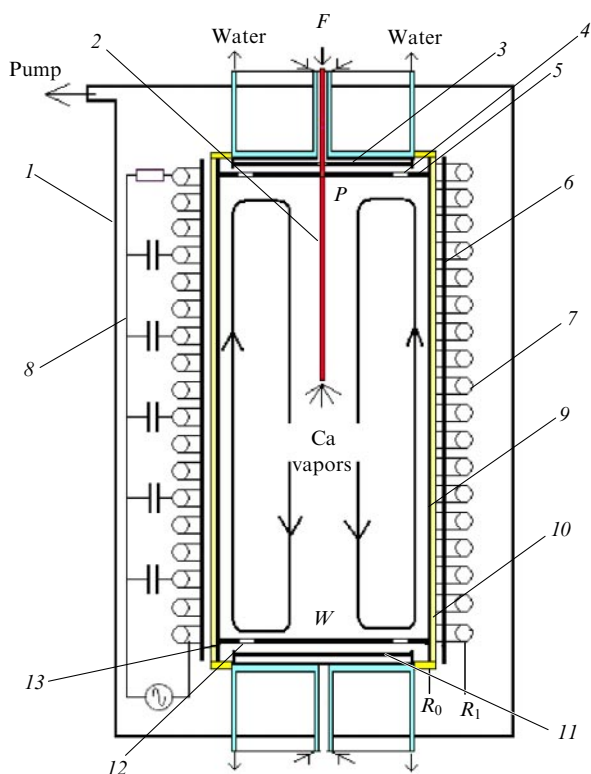


Figure 14. Schematic diagram of the installation for the separation of isotopes. 1—main vacuum chamber; 2—feed flow to the centrifuge; 3 and 11—water-cooled discs for the selection of heavy and light fractions; 4 and 12—openings through which the heavy and light fractions are extracted from the separation chamber; 5 and 13—hot ends of the chamber; 6—current-carrying rods that excite a rotating magnetic field; 7—delay line coils that create a traveling magnetic field; 8—delay line capacitors; 9—separation chamber wall; 10—cylindrical layer of high-temperature ceramics; R_0 is the inner radius of the separation chamber wall, R_1 is the radius of the winding of the traveling magnetic field, F is the feed flow, P is the selection flow, and W is the waste flow.

of the order of several kW, the plasma rotates at a velocity insufficient for effective separation in the field of centrifugal forces. However, the calculation performed in [69] showed that a way to increase the azimuthal velocity of the medium and the centrifugal effects of separation is to reduce the angular velocity of the field rotation $\omega_0 = 2\pi\nu$ while maintaining the power input into the discharge at a constant level. However, this requires the intensity of the alternating magnetic field, and, consequently, the currents in the winding to be increased. In [70], a new concept of a low-frequency ($\nu \approx 30$ kHz) countercurrent plasma centrifuge is described, which is based on the use of a traveling magnetic field to enhance the radial separation effect. It was proposed to rotate the plasma by a rotating magnetic field, and to create axial circulation due to a traveling magnetic wave. It is shown that, due to the favorable profile of the circulation flow created by the traveling magnetic field, a significant enhancement of the radial separating effect along the length of the device can be achieved. In [71–74], the feasibility of using an HF centrifuge to separate Ca and Li isotopes was numerically evaluated. Figure 14 shows a schematic of the facility under design with supply and extraction systems. Figure 15 shows the calculations of the maximum centrifuge separation coefficients with enhancement α as a function of the dimensionless output flow h in the case of separation of potassium and calcium isotopes.

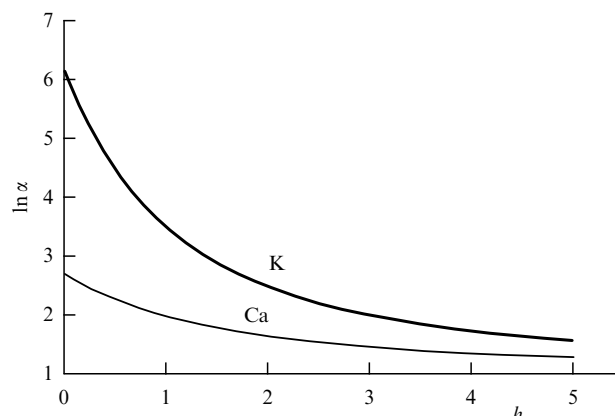


Figure 15. Logarithm of separation coefficient as a function of the dimensionless selection flow under optimal circulation.

The above results show that separation factors of the order of $\alpha \approx 2$ can be achieved in a plasma centrifuge with enhancement. The degree of enrichment can be increased further if more than one facility is used. Such an external cascading is possible, although it will require additional effort. However, the required number of stages connected in series is significantly reduced compared to that used in existing industrial methods.

In [75, 76], as applied to an HF plasma centrifuge, the hydrodynamic aspects of countercurrent excitation due to axial temperature gradients are considered. It is shown that, when one of the discharge chamber ends is cooled in a not very intense temperature regime, countercurrent axial circulation can be excited, which is necessary for the effective enhancement of the primary effect along the column length.

Study [77] presents a detailed review of approaches to the problem of reprocessing spent nuclear fuel (SNF). However, the task of separating chemical mixtures of various gases with a large relative mass difference is not directly related to the more challenging problem of obtaining stable isotopes. In this review, we only outline those recent results regarding the nuclear fuel reprocessing, which are not included in review [77], and relate to separation in a sufficiently dense plasma, where the enrichment effects occur due to mutual diffusion.

An original proposal on the use of a rotating plasma for SNF reprocessing was made in [78]. The idea of separating nuclear fuel from fission products was based on Okawa's plasma filter method. Unfortunately, this proposal failed to yield positive results in terms of the degree of separation. In our opinion, this method did not take into account the possibility of decelerating a rotating mixture by secondary flows associated with the influence of structural elements and spatial inhomogeneity of centrifugal forces. It was proposed in [79] to use a rotating magnetic field to create a low-frequency direct-flow plasma centrifuge designed to separate nuclear fuel from fission fragments. Due to the large differences among the masses of the separated components of the mixture, such a system makes it possible to use the primary radial separating effect, which is not possible in countercurrent devices.

Figure 16 shows a schematic diagram of a centrifuge based on a plasma jet spun by an HF field. The separation effect in a model binary mixture with atomic masses of 120 and 240 was estimated for specific parameters of the facility and properties of a fully ionized plasma. The hydrodynamic parameters of the rotating and expanding plasma column, the

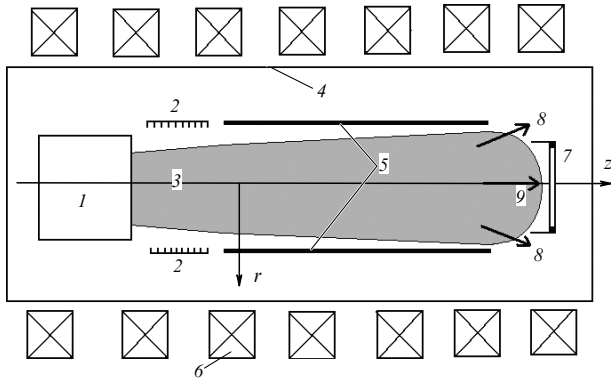


Figure 16. Schematic diagram of the device: 1—plasma source, 2—pockets, 3—plasma jet, 4—chamber, 5—current-carrying rods, 6—coils of a static magnetic field, 7—skimmer, 8—output of heavy fraction, 9—output of light fraction.

separating effect, and the performance of the device are estimated.

In [80, 81], a detailed calculation of the centrifugal field of an HF plasma centrifuge was carried out in the magneto-hydrodynamic approximation taking into consideration the Hall effect and in the multicomponent hydrodynamic approximation. For real plasma parameters with number density $n = 10^{18} \text{ m}^{-3}$, amplitude value of the HF field $B_0 = 2 \times 10^{-4} \text{ T}$, longitudinal confining magnetic field $B_z = 0.1 \text{ T}$, characteristic ion temperature $\langle T_i \rangle = 10^4 \text{ K}$, and mass difference of separated components $\Delta m = 2 \times 10^{-25} \text{ kg}$, the estimated values of the angular velocity of plasma rotation and the logarithm of the separation factor were $\Omega \approx 1.3 \times 10^5 \text{ s}^{-1}$ and $\ln \alpha \approx 10$, respectively [78]. It was shown in [81] that, if the central part is ‘cut out’ from a rotating plasma cylinder with a diameter of 10 cm using an annular skimmer with a diameter of about 2 cm, the concentration of the enriched fuel component in the extraction flow increases from the initial 0.96 to 0.999. The degree of extraction of fuel components is 0.93.

In [82], as applied to the problem of SNF reprocessing, the separation of a model Ag + Pb mixture was experimentally studied in a system with crossed radial electric and axial magnetic fields. The discharge voltage was 550 V, and the amperage varied in a range of 8–14 A. A plasma source based on an arc discharge with a hot cathode was used. The maximum separation factor of the mixture is shown to be as high as 8.

6. Energy consumption of diffusive plasma methods

Diffusive plasma methods of isotope separation in what regards the nature of the processes occurring in a weakly ionized plasma are similar to most modern industrial methods. For gas diffusive and centrifugal technologies, the specific energy consumption is usually determined. This value is the ratio of the power W consumed by the facility to its separating power δU . The specific energy consumption of various plasma methods was calculated in [83]. For a DC discharge, the specific energy consumption can be estimated according to the formula

$$\frac{W}{\delta U} \approx \frac{512 j_e k_B^2 T^2}{9\pi^2 \rho D \beta^2 e^2} \left(\frac{m}{\Delta m} \right)^2, \quad (16)$$

where j_e is the electron current density in the separation zone averaged over the cross section, T is the temperature of the neutral gas, β is the degree of mixture ionization, ρ is the plasma mass density, and D is the coefficient of mutual diffusion of the mixture components being separated. If the following characteristic values of the discharge parameters and plasma properties are used, $j_e = 10^6 \text{ A m}^{-2}$, $T = 10^3 \text{ K}$, $\rho D = 10^{-4} \text{ kg (m s)}^{-1}$, $\beta = 10^{-2}$, and $E = 10^3 \text{ V m}^{-1}$, we obtain

$$\frac{W}{\delta U} \approx 1200 \left(\frac{m}{\Delta m} \right)^2 \text{ kWh (SWU)}^{-1}. \quad (17)$$

In the case of an HF system with a traveling magnetic field, the expression for specific energy consumption takes the form

$$\frac{W}{\delta U} \approx \frac{128 L p_n^2 R^2 V_f^2}{\pi \rho D W} \left(\frac{m}{\Delta m} \right)^2, \quad (18)$$

where p_n is the average pressure of the neutral gas and V_f is the phase velocity of the wave. Taking as characteristic values of system parameters and plasma properties $L = 1 \text{ m}$, $R = 0.03 \text{ m}$, $p_n = 1 \text{ N m}^{-2}$, $V_f = 10^5 \text{ m s}^{-1}$, $W = 5 \times 10^3 \text{ W}$, $\rho D = 10^{-4} \text{ kg (m s)}^{-1}$, we find

$$\frac{W}{\delta U} \approx 200 \left(\frac{m}{\Delta m} \right)^2 \text{ kWh (SWU)}^{-1}. \quad (19)$$

In conclusion, we estimate the specific energy consumption of a plasma centrifuge with crossed radial electric and axial magnetic fields under conditions of weak ionization of the medium. If viscous dissipation and the logarithmic velocity profile ($V_\phi = V_0 \ln(r/R)$) predominate, the minimum value of specific energy consumption can be estimated using the formula

$$\frac{W}{\delta U_{\max}} \approx \frac{\pi}{12} \text{Sc} V_0^2 \left(\frac{m}{\Delta m} \right)^2, \quad (20)$$

where $\text{Sc} = \eta/(\rho D)$ is the Schmidt number. If we use the data on the experimentally achievable values of the plasma rotation velocity ($V_0 \approx 8 \times 10^3 \text{ m s}^{-1}$ and $\text{Sc} = 0.7$), the specific energy consumption in the separation of xenon isotopes can be estimated as

$$\frac{W}{\delta U_{\max}} \approx 3 \left(\frac{m}{\Delta m} \right)^2 \text{ kWh (SWU)}^{-1}. \quad (21)$$

Thus, in terms of energy consumption, a plasma centrifuge is potentially advantageous over a system with a traveling magnetic wave, especially in the case of a DC discharge.

As mentioned in the Introduction, plasma methods are universal. However, due to high energy consumption, they can only be competitive in the separation of isotopes of elements that do not have volatile components under normal conditions, where centrifugal technology is not applicable. Therefore, it is expedient to compare plasma methods with electromagnetic mass separation. The issue of productivity and energy consumption of a mass separator is described in detail in [84]. In relation to this, an important circumstance should be noted. In considering the effectiveness of the electromagnetic method, the concept of ‘separating power’ δU is usually not involved. In [84], data are given for energy

consumption per unit productivity of the electromagnetic method, expressed in $[\text{kWh mg}^{-1}]$. For example, in the particular case of obtaining the ^{168}Yb isotope, the ratio of the consumed power W to the extraction flow P_e was $W/P_e = 76 \text{ kWh mg}^{-1}$. We now endeavor to compare, at least approximately, the performance of plasma centrifugal and electromagnetic methods. The performance of an HF plasma centrifuge as applied to the separation of Ca isotopes was calculated in [71]. As follows from the results obtained, the concentration of the target ^{48}Ca isotope in the optimal mode of operation of the HF plasma centrifuge with a length of 1 m and a chamber radius of 0.05 m can be increased from 0.187% to 0.37%. The extraction flow is about $P_e \approx 1.6 \text{ mg s}^{-1}$ (power consumption is about 10 kW). In an electromagnetic separator [85], at an ion current of 60 mA (corresponding to an extraction flow of $P_e \approx 3 \times 10^{-2} \text{ mg s}^{-1}$), the concentration of ^{48}Ca increases from 0.187% to 87%. The above estimates show that the advantage of the electromagnetic method in terms of product purity is compensated in the plasma method by a significantly higher productivity. If we compare the separating capacities δU_e and δU_c of the electromagnetic and plasma methods, we obtain for $\langle \rho D \rangle R \approx 10^{-3} \text{ g s}^{-1}$ similar results: $\delta U_e \approx 2 \times 10^{-4} \text{ g s}^{-1}$ and $\delta U_c \approx 1.5 \times 10^{-4} \text{ g s}^{-1}$ [71].

It is worth noting that at present plasma methods are not used in the industrial production of isotopes. However, it can already be asserted that, in obtaining isotopes of elements that do not have suitable gaseous compounds at room temperature, plasma methods will be cost effective at intermediate scales of production, when the electromagnetic method becomes very expensive. The industrial implementation of plasma methods is possible where there is a demand for isotopes on a production scale of about 100 kg yr^{-1} or more. It is also possible that a combination of the plasma and electromagnetic methods will make it possible to significantly reduce the cost of the product if a plasma facility, which has a higher productivity, is used for preliminary enrichment of the mixture.

7. Conclusion

Numerous experimental and theoretical studies of isotope separation processes based on the selective diffusion of separated components in plasma are reviewed. Interest in these studies is due to the absence of convenient gaseous compounds in most elements, as a result of which the method of centrifugal cascades is not applicable. Based on the developed method for calculating diffusion processes in gas mixtures in the field of various kinds of external force fields, a theoretical explanation is provided for experimental data on the separation of isotopic mixtures in plasma separation devices. In the case of a system with a traveling magnetic field, it is shown that the main contribution to the separation of isotopes at high pressures is made by thermal diffusion, while at low pressures, by ionic wind and isotope cataphoresis. It has also been established that the driving mechanisms of separation in a direct DC discharge are isotope cataphoresis at low pressures and ionic wind at high pressures.

Experimental and theoretical studies of centrifugal separating effects in pulsed plasma centrifuges are discussed in detail. In a pulsed system with crossed fields, when hydrogen is added to the ^{20}Ne – ^{22}Ne isotope mixture to be separated, record high values of the centrifugal effect ($\epsilon \approx 34\%$) have

been achieved. As applied to stationary systems, various mechanisms that enhance the centrifugal effect are discussed. The concept of multiple enhancement of the separation effect along the length of the device is substantiated. The conditions are determined under which an effective enhancement of the radial effect in a stationary plasma centrifuge can be attained. The feasibility of using high-frequency fields for the implementation of centrifugal radial separation effects and their enhancement due to countercurrents are considered. The specific energy consumption of various plasma diffusion methods is estimated and the potential advantage of centrifuges is pointed out. In conclusion, the calculated values of the selection flows in an HF plasma centrifuge are compared with the experimental data on the performance of an electromagnetic separator. A conclusion is made that the plasma method can be used for the separation of isotopes of those elements that do not have volatile compounds under normal conditions, at intermediate scales of production.

References

1. Benedict M, Pigford T H *Nuclear Chemical Engineering* (New York: McGraw-Hill, 1957); Translated into Russian: *Khimicheskaya Tekhnologiya Yadernykh Materialov* (Moscow: Atomizdat, 1960)
2. Sosnin L J et al. *Nucl. Instrum. Meth. Phys. Res. A* **334** 41 (1993)
3. JSC Production Holding "Elektrokhimicheskii Zavod", Zelenogorsk, Krasnoyarsky krai, Russia, <http://www.ecp.ru>
4. Potanin E P, Sosnin L Yu, Chel'tsov A N *Atom. Energy* **127** 153 (2020); *Atom. Energ.* **127** (3) 140 (2019)
5. Kashcheev N A, Dergachev V A *Elektromagnitnoe Razdelenie Izotopov i Izotopnyi Analiz* (Electromagnetic Separation of Isotopes and Isotopic Analysis) (Moscow: Energoatomizdat, 1989)
6. Demirkhanov R A et al., in *3-ya Vsesoyuznaya Konf. po Plazmennym Uskoritelyam*, Minsk, 12–14 Maya, 1976 g., *Tezisy Dokladov* (Proc. of the 3rd All-Russian Conf. on Plasma Accelerators, Minsk, May 12–14, 1976, Abstracts) (Ed. A I Morozov) (Minsk: Institut Fiziki, 1976) p. 198
7. Matsumura Y, Abe T *Jpn. Appl. Phys.* **19** L457 (1980)
8. Bonnevier B *Ark. Fys.* **33** 255 (1966)
9. Askarian G A, Namiot V A, Rukhadze A A *Sov. Tech. Phys. Lett.* **1** 356 (1975); *Pis'ma Zh. Tekh. Fiz.* **1** 820 (1975)
10. Dawson J M et al. *Phys. Rev. Lett.* **37** 1547 (1976)
11. Dolgolenko D A, Muromkin Yu A *Phys. Usp.* **52** 345 (2009); *Usp. Fiz. Nauk* **179** 369 (2009)
12. Potanin E P *Inzh.-Fiz. Zh.* **39** 811 (1980)
13. Potanin E P *Zh. Tekh. Fiz.* **53** 1717 (1983)
14. Potanin E P *Zh. Tekh. Fiz.* **54** 803 (1984)
15. Zhdanov V M, Karchevskii A I, Potanin E P *Pis'ma Zh. Tekh. Fiz.* **4** 507 (1978)
16. Potanin E P, Preprint No. 4635/12 (Moscow: Kurchatov Institute of Atomic Energy, 1988)
17. Potanin E P *Tech. Phys.* **38** 546 (1993); *Zh. Tekh. Fiz.* **63** (7) 28 (1993)
18. Potanin E P *Razdelenie Izotopov v Plazme Statsionarnykh Dugovykh i VCh-Razryadov* (Separation of Isotopes in a Plasma of Stationary Arc and HF Discharges) (Progress in Science and Technology. Plasma Physics, Vol. 12, Ed. A I Karchevskii) (Moscow: VINITI, 1991)
19. Karchevskii A I et al., in *3-ya Vsesoyuznaya Konf. po Plazmennym Uskoritelyam*, Minsk, 12–14 Maya, 1976 g., *Tezisy Dokladov* (Proc. of the 3rd All-Russian Conf. on Plasma Accelerators, Minsk, May 12–14, 1976, Abstracts) (Ed. A I Morozov) (Minsk: Institut Fiziki, 1976) p. 201
20. Karchevskii A I et al. *Fiz. Plazmy* **3** 409 (1977)
21. Chapman S, Cowling T G *The Mathematical Theory of Non-uniform Gases; an Account of the Kinetic Theory of Viscosity, Thermal Conduction, and Diffusion in Gases* (Cambridge: Univ. Press, 1952); Translated into Russian: *Matematicheskaya Teoriya Neodnorodnykh Gazov* (Mathematical Theory of Inhomogeneous Gases) (Moscow: IL, 1960)
22. Rozen A M *Teoriya Razdeleniya Izotopov v Kolonnakh* (Theory of Isotope Separation in Columns) (Moscow: Atomizdat, 1960)

23. Nikolaev B I et al. *Sov. Atom. Energy* **24** 604 (1968); *Atom. Energ.* **24** 485 (1968)
24. Smirnov B M *Sov. Phys. Usp.* **10** 313 (1967); *Usp. Fiz. Nauk* **92** 75 (1967)
25. Radtsig A A, Smirnov B M *High Temp. Sci.* **14** 611 (1977); *Teplofiz. Vys. Temp.* **14** 686 (1976)
26. Karchevskii A I, Potanin E P *Sov. Phys. Tech. Phys.* **23** 1197 (1978); *Zh. Tekh. Fiz.* **48** 2097 (1978)
27. Karchevsky A I, Potanin E P *J. Phys. Colloq.* **7** C7-213 (1979)
28. Karchevskii A I, Potanin E P *Zh. Tekh. Fiz.* **50** 433 (1980)
29. Karchevskii A I, Potanin E P *Sov. J. Plasma Phys.* **7** 171 (1981); *Fiz. Plazmy* **7** 318 (1981)
30. Gorbunova E F et al. *Pis'ma Zh. Tekh. Fiz.* **4** 7161 (1978)
31. Karchevskii A I, Potanin E P *Sov. J. Plasma Phys.* **8** 553 (1982); *Fiz. Plazmy* **8** 1781 (1982)
32. Karchevsky A I, Potanin E P, in *Proc. of the XV Intern. Conf. Phenomena in Ionized Gases, Minsk, USSR, July 14–18, 1981*, Pt. 2, p. 1230
33. Babichev A P et al. *Pis'ma Zh. Tekh. Fiz.* **5** 1149 (1979)
34. Gorbunova E F, Karchevskii A I, Muromkin Yu A *Sov. J. Plasma Phys.* **12** 625 (1986); *Fiz. Plazmy* **12** 1087 (1986)
35. Gorbunova E F et al., in *XVI Intern. Conf. Phenomena in Ionized Gases, Düsseldorf, Fed. Rep. of Germany, 29 August–2 September 1983* (Eds W Botticher, H Wenk, E Schultz-Gulde) (Düsseldorf: Düsseldorf Univ. Inst. Theor. Phys., 1983) p. 492
36. Ezoubtchenko A et al. *Plasma Sources Sci. Technol.* **7** 136 (1998)
37. Karchevskiy A I, Potanin E P *Sov. J. Plasma Phys.* **8** 101 (1982); *Fiz. Plazmy* **8** 178 (1982)
38. Duman E L et al. *Sov. J. Plasma Phys.* **17** 127 (1991); *Fiz. Plazmy* **17** 216 (1991)
39. Gorbunova E F et al. “Isotope separation in the positive column of a direct current discharge” (1983), https://www.researchgate.net/publication/241215872_Isotope_Separation_in_the_Positive_Column_of_a_Direct_Current_Discharge
40. Bonnevier B *Plasma Phys.* **13** 763 (1971)
41. James B M, Simpson S W *Phys. Lett. A* **46** 347 (1974)
42. Cairns J B S, in *Uranium Isotope Separation Intern. Conf., London, 1975* Vol. 9 (London: British Nuclear Energy Society, 1975) p. 1
43. Belorusov A V et al. *Sov. Tech. Phys. Lett.* **2** (7) 260 (1976); *Pis'ma Zh. Tekh. Fiz.* **2** 664 (1976)
44. Belorusov A V et al. *Pis'ma Zh. Tekh. Fiz.* **6** 358 (1980)
45. Korobtsev S V et al. *Sov. Phys. Dokl.* **28** 504 (1983); *Dokl. Akad. Nauk SSSR* **270** 876 (1983)
46. Korobtsev S V, Rusanov V D *Plazmennaya Tsentrifuga — Plazmo-Khimicheskii Reaktor Novogo Tipa* (Plasma Centrifuge: Plasma-Chemical Reactor of a New Type) A Review (Moscow: TsNIIatom-inform, 1988)
47. Fetterman A J, Fisch N J *Phys. Plasmas* **18** 094503 (2011)
48. Belorusov A V, Karchevskii A I, Potanin E P, Ustinov A L *Zh. Tekh. Fiz.* **50** 450 (1980)
49. Nathrath N, in *Proc. of the 13th Intern. Conf. on Phenomena in Ionized Gases, Berlin, GDR, September 12–17, 1977* (Leipzig: Physical Society of the GDR, 1977) p. 697
50. Babaritskii A I et al. *Fiz. Plazmy* **4** 842 (1978)
51. Ivanov A A, Leiman V G *Fiz. Plazmy* **4** 668 (1978)
52. Ivanov A A, Leiman V G *Fiz. Plazmy* **9** 786 (1983)
53. Geva M, Krishnan M, Hirshfield J L *J. Appl. Phys.* **56** 1398 (1984)
54. Ikehata T et al., in *12th Intern. Conf. on Electromagnetic Isotope Separators and Techniques Related to their Applications, September 2–6, 1991, CYRIC, Japan*
55. Del Bosco E, Dallaqua R S, Simpson S W, in *Fifth Workshop on Separation Phenomena in Liquids and Gases, SPLG, Brasil, 22–26 September 1996*, p. 26
56. Kurko O V, Mikhailovskii A B, Preprint No. 3619/6 (Moscow: Kurchatov Institute of Atomic Energy, 1982)
57. Karchevskii A I, Potanin E P, Sazykin A A *Fiz. Plazmy* **5** 1355 (1979)
58. Donskoi K V, Drobyshevskii E M, Nazarov E V *Zh. Tekh. Fiz.* **33** 1328 (1963)
59. Zhdanov V M, Karchevskii A I, Potanin E P, Ustinov A L *Zh. Tekh. Fiz.* **49** 1879 (1979)
60. Potanin E P *Fiz. Plazmy* **9** 1322 (1983)
61. Karchevsky A I, Potanin E P, in *XVII Intern. Conf. on Phenomena in Ionized Gases, Budapest, 8–12 July 1985*, Pt. 1, p. 20
62. Karchevskii A I et al. *Fiz. Plazmy* **8** 306 (1982)
63. Potanin E P, Ustinov A L *Fiz. Plazmy* **10** 1040 (1984)
64. Leskov L V et al., in *3-ya Vsesoyuznaya Konf. po Plazmennym Uskoritelyam, Minsk, 12–14 Maya, 1976 g., Tezisy Dokladov* (Proc. of the 3rd All-Russian Conf. on Plasma Accelerators, Minsk, May 12–14, 1976, Abstracts) (Ed. A I Morozov) (Minsk: Institut Fiziki, 1976) p. 216
65. Potanin E P, Karchevskii A I, Ustinov A L *Zh. Tekh. Fiz.* **48** 472 (1978)
66. Belorusov A V et al. *Fiz. Plazmy* **5** 1239 (1979)
67. Borisevich V, Potanin E, Whichello J V *IEEE Trans. Plasma Sci.* **48** 3472 (2020)
68. Demirkhanov R A et al., in *3-ya Vsesoyuznaya Konf. po Plazmennym Uskoritelyam, Minsk, 12–14 Maya, 1976 g., Tezisy Dokladov* (Proc. of the 3rd All-Russian Conf. on Plasma Accelerators, Minsk, May 12–14, 1976, Abstracts) (Ed. A I Morozov) (Minsk: Institut Fiziki, 1976) p. 197
69. Averin V G et al. *Zh. Tekh. Fiz.* **48** 66 (1978)
70. Borisevich V D, Potanin E P *Phys. Scr.* **92** 075601 (2017)
71. Borisevich V D, Potanin E P, Whichello J V *Phys. Plasmas* **25** 113503 (2018)
72. Borisevich V D, Potanin E P *Tech. Phys. Lett.* **44** 1195 (2018); *Pis'ma Zh. Tekh. Fiz.* **45** (1) 8 (2019)
73. Borisevich V D, Potanin E P *Tech. Phys.* **63** 768 (2018); *Zh. Tekh. Fiz.* **88** 791 (2018)
74. Borisevich V D, Potanin E P, Whichello J V *Sep. Sci. Technol.* **55** 1829 (2020)
75. Whichello J V, Borisevich V D, Potanin E P *J. Appl. Phys.* **130** 045106 (2021)
76. Borisevich V D, Potanin E P, Whichello J V *Sep. Sci. Technol.* **56** 2141 (2021)
77. Dolgolenko D A, Muromkin Yu A *Phys. Usp.* **60** 994 (2017); *Usp. Fiz. Nauk* **187** 1071 (2017)
78. Litvak A et al., in *Proc. of the 30th European Physical Society Conf. on Controlled Fusion and Plasma Physics, St. Petersburg, Russia, 7–11 July 2003* Vol. 27 (London: ECA, 2003) p. O1.6A
79. Gorshunov N M, Potanin E P *Atom. Energy* **124** 197 (2018); *Atom. Energ.* **124** 164 (2018)
80. Gorshunov N M, Potanin E P *Tech. Phys.* **65** 461 (2020); *Zh. Tekh. Fiz.* **90** 482 (2020)
81. Gorshunov N M, Potanin E P *Plasma Phys. Rep.* **46** 147 (2020); *Fiz. Plazmy* **46** 110 (2020)
82. Liziakin G D et al. *J. Phys. D* **54** 414005 (2021)
83. Potanin E P, Doctoral Dissertation in Physics and Mathematics (Moscow: Kurchatov Institute of Atomic Energy, 1997)
84. Baranov V Yu (Ed.) “Elektromagnitnyi i plazmennyy metod” (“Electromagnetic and plasma method”), in *Izotopy: Svoystva, Poluchenie, Primenenie* (Isotopes: Properties, Production, Application) (Moscow: IzdAT, 2000) Ch. 6, p. 237
85. Kabanov I A *Perspektiv. Mater.* **10** (Topical issue) 86 (2011)